Published in final edited form as:

Cancer Res. 2016 November 15; 76(22): 6669–6679. doi:10.1158/0008-5472.CAN-16-0571.

Comparative analysis of bispecific antibody and streptavidin-targeted radioimmunotherapy for B cell cancers

Damian J. Green[1,2], **Shani L. Frayo**[1], **Yukang Lin**[1], **Donald K. Hamlin**[3], **Darrell R. Fisher**[4], **Sofia H.L. Frost**[1], **Aimee L. Kenoyer**[1], **Mark D. Hylarides**[1], **Ajay K. Gopal**[1,2], **Theodore A. Gooley**[1], **Johnnie J. Orozco**[1,2], **Brian G. Till**[1], **Shyril O'Steen**[1], **Kelly D. Orcutt**[5], **D. Scott Wilbur**[3], **K. Dane Wittrup**[5], and **Oliver W. Press**[1,2]

[1]Clinical Research Division, Fred Hutchinson Cancer Research Center, Seattle, Washington, USA

[2]Department of Medicine, University of Washington, Seattle, Washington, USA

[3]Department of Radiation Oncology, University of Washington, Seattle, Washington, USA

[4]Dade Moeller Health Group, Richland, Washington, USA

[5]Departments of Chemical Engineering and Biological Engineering, Massachusetts Institute of Technology

Abstract

Streptavidin (SA)-biotin pretargeted radioimmunotherapy (PRIT) that targets CD20 in non-Hodgkin lymphoma (NHL) exhibits remarkable efficacy in model systems, but SA immunogenicity and interference by endogenous biotin may complicate clinical translation of this approach. In this study, we engineered a bispecific fusion protein (FP) that evades the limitations imposed by this system. Briefly, one arm of the FP was an anti-human CD20 antibody (2H7) with the other arm of the FP an anti-chelated radiometal trap for a radiolabeled ligand (yttrium[Y]-DOTA) captured by a very high-affinity anti-Y-DOTA scFv antibody (C825). Head-to-head biodistribution experiments comparing SA-biotin and bispecific FP (2H7-Fc-C825) PRIT in murine subjects bearing human lymphoma xenografts demonstrated nearly identical tumor targeting by each modality at 24 hrs. However, residual radioactivity in the blood and normal organs was consistently higher following administration of 1F5-SA compared to 2H7-Fc-C825. Consequently, tumor-to-normal tissue ratios of distribution were superior for 2H7-Fc-C825 ($p<0.0001$). Therapy studies in subjects bearing either Ramos or Granta subcutaneous lymphomas demonstrated that 2H7-Fc-C825 PRIT is highly effective and significantly less myelosuppressive than 1F5-SA ($p<0.0001$). All animals receiving optimal doses of 2H7-Fc-C825 followed by ^{90}Y-DOTA were cured by 150 days, whereas the growth of tumors in control animals progressed rapidly with complete morbidity by 25 days. In addition to demonstrating reduced risk of immunogenicity and an absence of endogenous biotin interference, our findings offer a preclinical proof of concept for the preferred use of bispecific PRIT in future clinical trials, due to a slightly superior biodistribution profile, less myelosuppression and superior efficacy.

Corresponding Author: Damian J. Green, M.D., Clinical Research Division, Fred Hutchinson Cancer Research Center, 1100 Fairview Avenue N., MS: D3-190, Seattle, WA 98109, (206) 667-5398 (Office), (206) 667-1874 (Fax), dgreen@fhcrc.org.

Disclosure of COI: KDR and KDO hold U.S. patent 8,648,176 (Engineered Proteins with High Affinity for DOTA Chelates). The authors have no other conflicts of interest to disclose.

Keywords

Radioimmunotherapy; lymphoma; CD20; pretargeting; preclinical

INTRODUCTION

An estimated 19,970 Americans died of Non-Hodgkin Lymphoma in 2015(1), despite the availability of modern immunochemotherapy regimens and the introduction of novel agents such as ibrutinib and idelalisib.(2,3) This statistic emphasizes the need for additional improvements in the therapeutic armamentarium for lymphomas. One promising approach is to exploit the specificity of monoclonal antibodies to target drugs, toxins, or radionuclides to lineage-specific cell surface antigens present on B cell malignancies.(4,5) Early studies with "first generation" radiolabeled antibodies targeting the CD20 antigen, such as ^{131}Iodine-tositumomab and ^{90}Yttrium-ibritumomab tiuxetan, induced objective tumor responses in 60–80% of patients with relapsed or refractory indolent B cell malignancies(4,6), and in 80–100% of patients treated in the front-line setting,(7,8) leading to United States Food and Drug Administration (FDA) approval of both radioimmunoconjugates. Despite the unequivocal efficacy and safety of these agents, they have been under-utilized, resulting in withdrawal of ^{131}Iodine-tositumomab from the commercial market. Although the reasons for the under-utilization of radioimmunotherapy (RIT) are controversial, it appears likely that the simultaneous emergence of other promising agents (e.g. bendamustine, ibrutinib, idelalisib) which were logistically easier to administer in the offices of hematologists and oncologists, put RIT at a competitive disadvantage. However, despite their convenience and demonstrated short-term efficacy none of these new agents have curative potential, at least as single agents. First generation RIT often achieves disease control, however, low tumor-to-normal organ ratios of absorbed radioactivity (1.5:1 for tumor-to-lung and 10:1 for tumor-to-whole body following ^{131}I-anti-CD20) do not reliably lead to disease eradication.(9) The majority of patients treated at conventional doses of anti-CD20 RIT eventually relapse.(10) While myeloablative RIT conditioning for autologous stem cell transplant (ASCT) has led to objective remission rates of 85–95%, at least 1/3 of patients with NHL still relapse, 3–5% of patients die of infections or pneumonitis and nonhematopoietic toxicities can be significant.(9,11–16) Advances in RIT that markedly improve the efficacy, and diminish the toxicity of the approach, would potentially elevate the attractiveness of RIT, despite its logistic challenges. The development and optimization of multi-step "pretargeted" radioimmunotherapy (PRIT) approaches appear particularly promising.

Several PRIT methods have been developed, all of which have been shown to be markedly superior to conventional RIT with directly radiolabeled antibodies.(17–22) All of these strategies administer a derivatized lymphoma-reactive antibody in a non-radioactive form, allowing it to localize to tumor sites and accumulate without subjecting the rest of the body to nonspecific irradiation. After maximal accumulation of antibody in the tumor, a low molecular weight radioactive moiety with a high affinity for the derivatized tumor-reactive antibody is administered. The small size of the second reagent facilitates rapid tumor penetration, capture and retention by the pre-targeted antibody. Unbound molecules of the radioactive second reagent are so small that they are rapidly cleared from the blood and

excreted in the urine. In some PRIT approaches, a “clearing agent” (CA) is injected shortly before the radiolabeled small molecule to accelerate removal of residual unbound antibody from the bloodstream, preventing it from complexing with the radiolabeled second step reagent (Figure 1).

Technologies employed to facilitate high-avidity association of the radiolabeled second step reagent with the pretargeted tumor-bound antibody include streptavidin-biotin (SA-biotin) approaches, bispecific monoclonal antibodies, complementary hybridization (Watson–Crick pairing) of phosphorodiamidate morpholino DNA oligomers(23,24), and trans-cyclooctene-modified antibodies (Abs) binding to radiolabeled tetrazine ligands.(25,26) Although each of these PRIT methods has been shown to be superior to “first generation” RIT with directly radiolabeled antibodies, no head-to-head comparisons have been conducted to discern which of the PRIT approaches is most promising for clinical development. Here, we present a comparative analysis of the biodistribution and therapeutic efficacy of the two most popular PRIT strategies, SA-biotin and bispecific antibody targeting (Figure 1). As demonstrated in this report, both approaches are highly promising, though biodistributions of radioactivity favor the bispecific antibody approach. Each PRIT method was capable of curing 70–100% of animals bearing lymphoma xenografts when used under optimal conditions, but the bispecific antibody method produced less hematologic toxicity than SA-biotin PRIT. Expected reduced immunogenicity, and absence of potential interference from endogenous biotin-blocking, also argue in favor of the bispecific antibody approach over SA-biotin PRIT for future clinical trials.

MATERIALS AND METHODS

Construction of a bispecific 2H7-Fc-C825 (anti-CD20 x anti-Y-DOTA) fusion gene

A pDG expression vector containing a 2H7-hIgG1-hRNase gene under the control of the CMV promoter was provided by Jeffrey Ledbetter (Univ. of Washington). An anti-yttrium-DOTA 2D12.5 scFv was supplied by Claude Meares (Univ. of California Davis). A plasmid harboring a C825 ds-scFv gene, an affinity-improved 2D12.5 antibody, was obtained from Dane Wittrup (MIT) (27,28). An EcoRV-XbaI fragment of 2D12.5 was cloned into the pDG expression vector generating an O22-3-9 plasmid. An EcoRV-XbaI fragment of C825 was inserted into the plasmid O22-3-9 resulting in an O89-1-6 construct carrying 2H7-Fc-C825.

Isolation of CHO cell clones stably expressing 2H7-Fc-C825

The AscI-linearized O89-1-6 DNA (250μg) was mixed with $2x10^7$ CHO-DG44 cells and electroporated at 280V, 950 microFarads. Transfected cells were incubated in non-selective media overnight and plated in 96-well plates in Excell 302 complete CHO media (CCM) containing 50nM methotrexate (Sigma). Clones with the highest expression of the FP, determined by an IgG sandwich ELISA, were further treated using progressively increasing concentrations of methotrexate, (50nM to 500nM).

Expression and purification of the 2H7-Fc-C825

One of the highest expressing clones, 16B12/300, was thawed (10^7 cells) and expanded into 40 T175 flasks with 100ml per flask CCM plus 300nM MTX at an initial density of $1x10^5$

cells/ml and incubated for 14 days. Supernatants were purified over a 12-ml protein A-agarose column (RepliGen Bio Processing). The fractions containing the FP were pooled, dialyzed, and sterile filtered. A non-binding control bispecific anti-Tag72 CC49-Fc-C825 FP was produced using the same methods.

Synthesis of a DOTAY-dextran (DYD) CA for use with the 2H7-Fc-C825 fusion protein

Amino dextran 500kDa, 30.5mg, (Life Technologieswas reacted with 6.1mg of DOTA-–benzyl-NCS (MW=697kDa) and 11.4μl of triethylamine overnight,(28), diluted in sodium acetate pH 5.2 and 100 equivalents of yttrium nitrate (336mg) and incubated overnight at 37°C. The mixture was dialyzed against 2L of water for 3 days, dried on a Biotage V10 evaporator, dissolved in 2ml PBS,passed twice over a BioRad EconoPak 10DG column, dialyzed against water for 5 days, dried, weighed and. re-suspended in saline at 4 mg/ml and sterile filtered.

Streptavidin-biotin pretargeting reagents

Conjugates of the 1F5 anti-CD20 monoclonal antibody and SA were synthesized, purified and characterized as previously published.(29, 30) A synthetic, dendrimeric CA containing 16 *N*-acetylgalactosamine residues and a single biotin residue per molecule (NAGB) was obtained from Aletheon Pharmaceuticals (Seattle, WA) for use with the 1F5-SA conjugate.

Radiolabeling of DOTA-biotin with ^{90}Yttrium

^{90}Y labeling of DOTA-Biotin was performed using 12mg/mL DOTA-Biotin, 500mM ammonium acetate pH 5.3 and ^{90}Y heated for 60 minutes at 84°C. After cooling, 100mM DTPA was added and labeling efficiency determined using avidin-agarose beads.

Cell culture

The human Ramos (Burkitt lymphoma) cell line was obtained from the American Type Culture Collection (ATCC, Bethesda, MD; 2012). Granta-519 (mantle cell lymphoma; 2012) was obtained from Deutsche Sammlung von Mikroorganismen und Zellkulturen (DSMZ; Braunschweig, Germany). The EL4 and EL4-CD20 cell lines were gifts from Dr. Martino Introna and J. Golay, (Milan, Italy; obtained from ATCC; 2004). Cells were passaged twice, frozen and stored in liquid nitrogen. Fresh vials of cells were thawed and grown in log phase growth in RPMI 1640 medium supplemented with 10% fetal bovine serum in a 5% CO_2 incubator. Cell viability exceeded 95% by trypan blue exclusion. Mycoplasma testing (indirect DAPI stain and PCR testing) was performed on all cell lines prior to storage; in addition cell lines maintained in culture were tested on a rotating schedule. The Granta-519^{luc} cell line expressing firefly luciferase was created by transducing Granta-519 cells with the G-RV-FFLUC-Thy1.1-Neo plasmid as previously described.(31)

Cell binding analysis of antibody constructs

Ramos cells were concentrated and plated at a density of 10^6cells/well in a 96-well plate. Cells were blocked with non-binding antibody (negative control, HB8181), or an anti-CD20 antibody (1F5) at 50X the concentration of FPs and incubated for 45 minutes on ice. The FPs were added at 14x saturation of the CD20 binding sites, incubated for 45 minutes on ice,

washed and incubated with a 0.5X saturation ^{90}Y-DOTA-biotin for 45 minutes. Cells were washed to remove unbound ^{90}Y-DOTA-biotin and cell pellets counted on a Perkin Elmer Wizard 2480 gamma counter. The percent bound radioactivity was calculated as bound CPM divided by applied total CPM.

Mouse xenograft models

Athymic female mice (6–8 weeks old) (Harlan Sprague-Dawley) were housed in the FHCRC animal facility according to the Institutional Animal Care and Use Committee. All mice were placed on a biotin-deficient diet (Purina Mills) 7 days prior to PRIT studies. Ramos, Granta-519, or Granta-519^{luc} cells (10^7) were injected subcutaneously in the right flank 7–14 days prior to experiments to produce lymphoma xenografts measuring 6 to 8mm in diameter. Anti-asialoGM1 antiserum (30 μl, WAKO) was injected i.p. 8 days and 3 days prior to FP injection, and weekly for 100 days to prevent spontaneous tumor regressions.

Blood clearance studies

Groups of 3–5 athymic nude mice bearing Ramos or Granta-519 flank tumors were injected i.v. with 0.14 to 2.8nmol of 2H7-Fc-C825 followed 23-hours later by either 5.8nmol of NAGB or 5–32μg of DOTAY-Dextran (DYD) CA. Two micrograms of ^{90}Y-DOTA-biotin were injected one hour later. Retro-orbital blood sampling was performed at serial time points up to 24-hours. ^{90}Y was counted on a calibrated gamma counter and the percent of the injected dose per gram (%ID/g) present in blood was calculated.

Biodistribution studies

Groups of 3–5 mice with similar-sized tumors were injected i.v. with 0.14 to 2.8nmol of 2H7-Fc-C825, CC49-Fc-C825, HB8181-SA, or 1F5-SA. Twenty-three-hours later, mice were injected with 5.8nmol of NAGB CA (50μg) or 5μg of DYD CA, followed 1-hour later by 1.2nmol DOTA-biotin labeled with 20 to 40μCi (0.74–1.48MBq) of ^{90}Y. Blood, tumors, and body organs were obtained and ^{90}Y activity was measured using a calibrated system.

Radiation absorbed doses to organs and tissues

Mean values of radioactivity in organs and tissues for groups animals in biodistribution studies were plotted against time after injection and integrated to determine the total number of radioactive disintegrations in each major organ or tissue. Time-activity curves were integrated through complete decay of ^{90}Y. Radiation absorbed doses to organs and tissues were calculated from the integrated time-activity curves using the method of Hui, which accounts for organ mass, specific absorbed energy fraction, the beta-emission spectrum of ^{90}Y, and the beta-particle absorbed fractions for small organs(32). Average carcass values were estimated by blending the remains after tissue harvest. The results were expressed as radiation absorbed dose (cGy) per unit administered activity (μCi).

Therapy studies

The therapeutic efficacies of ^{90}Y-PRIT using SA-biotin and bispecific methods were evaluated in groups of 10 mice at each dose level. Groups of mice with similar sized, palpable tumors were randomized for the studies. Mice were given 1.4 or 2.8nmol of 2H7-

Fc-C825, 1F5-SA, or the non-binding, negative control antibodies, CC49-FC-C825 or HB8181-SA, followed by optimized doses of CA (5.8nmol for NAGB or 5μg DYD) 23-hours later. A single dose of 1.2nmol of DOTA-biotin labeled with 14.8–37MBq (400–1000μCi) ^{90}Y was administered 1 hour after the CA. Mice were assessed every 2 days for tumor volume, weight changes, and general appearance. Blood was sampled before therapy and 5, 12, 20, 30, 50 and 150 days after ^{90}Y administration to measure the leukocyte and platelet counts as well as hemoglobin and hematocrit values. Serum was collected before therapy, and 12, 20, 30, 50 and 150 days after therapy, to assess changes in aspartate aminotransferase (AST), alanine aminotransferase (ALT), creatinine, and blood urea nitrogen (BUN) levels. Bioluminescent tumor imaging was performed on mice bearing Granta-519^{luc} xenografts. Mice were injected i.p. with 10μL/g (15mg/mL) D-luciferin (Caliper Lifesciences, Hopkinton, MA) and imaged 10 minutes later on an IVIS Spectrum device. Mice were euthanized if xenografts exceeded 1200mm^3, caused obvious discomfort or impaired ambulation, or if mice lost more than 30% of their baseline body weight.

Statistical considerations

Differences between treatment groups in absorbed radiation dose and blood counts were determined using Student's t-tests. Tumor growth rate differences were determined using repeated measures analysis of variance, and survival differences were plotted by the Kaplan-Meier method(33) and compared using log-rank tests. Analyses were performed using GraphPad Prism 6 and JMP 12.2.0 (SAS Institute).

RESULTS

Engineering, expression, purification and in vitro testing of the 2H7-Fc-C825 FP

A bispecific antibody recognizing the B cell specific CD20 surface antigen as well the Yttrium-DOTA ligand was prepared by fusing the cDNAs encoding the scFv domain of the 2H7 anti-CD20 monoclonal antibody with the scFv of the affinity-enhanced C825 antibody, joined by a human IgG1 CH2-CH3 Fc hinge region and an NLG linker, as described above and illustrated in Figure 2A. The fusion gene construct was transfected into CHO-DG44 cells, and high-expressing clones were selected with methotrexate. The expressed 80-kDa monomeric protein spontaneously dimerized to a 160-kDa product, that was purified from culture supernatants using a protein A column and characterized by SDS-PAGE (Figure 2B). The purified bispecific antibody bound avidly to CD20-expressing target cells (i.e. EL4 murine T cells transfected with human CD20, [Figure 2C] and human lymphoma cell lines such as Ramos and Granta [Supplemental Figure S1]), but not to control cells (EL4) lacking CD20 expression (Figure 2C). The 2H7-Fc-C825 FP also avidly bound the Y-DOTA ligand in a concentration-dependent fashion, as demonstrated in a sandwich ELISA assay (Figure 2D).

In vivo pharmacokinetics and blood clearance of the 2H7-Fc-C825 FP

Pharmacokinetic analysis of the 2H7-Fc-C825 FP was challenged by an inability to radioiodinate the bispecific molecule without impairing its binding function. To circumvent this limitation, in vivo PK and blood clearance were performed by first injecting the unlabeled 2H7-Fc-C825 FP with or without administration of various doses of DYD CA 23-

hours later, followed by injection of 2.4nmol of ^{90}Y-DOTA-Biotin one-hour later. Blood was collected at various time intervals (0.08, 0.25, 0.5, 1, 2, 4 and 24-hours) following injection of radioactivity. The pharmacokinetics of various doses of bispecific antibody (0.14, 0.35, 0.7, 1.4, or 2.8nmol) labeled with ^{90}Y-DOTA-Biotin in the absence of CA are shown in Supplemental Figure S2. Dose-dependent levels of circulating radioimmunoconjugate were observed ranging from 14.7±1.4 %ID/g (23-hours after 2.8nmol bispecific Ab) to 0.6±0.4%ID/g ID/g (23-hours after 0.14nmol Ab), with a very slow blood clearance in the absence of DYD CA (t½ beta of ~44-hours with 1.4nmol of 2H7-Fc-C825). In contrast, DYD CA was highly effective at rapidly clearing >98% of circulating FP from the bloodstream within 30 minutes of administration at all doses tested (Figure 3A).

In vivo biodistributions of radioactivity following CD20 PRIT with the 2H7-Fc-C825 FP

The biodistributions of various doses (0.14, 0.35, 0.7, 1.4, or 2.8nmol) of 2H7-Fc-C825 bispecific Ab followed by trace-labeled ^{90}Y-DOTA were initially assessed in the blood, Ramos tumor xenografts and in critical normal organs in the absence of CA. Dose-dependent accumulation of radioactivity (up to 11.9%ID/g) was demonstrated in tumor sites 48-hours after injection of 2.8nmol of bispecific Ab (23-hours after injection of ^{90}Y-DOTA) (Supplemental Figure S3) and subsequent experiments optimized the system by assessing the impact of various doses of DYD CA. Athymic mice were injected with 1.4nmol of 2H7-Fc-C825 followed 23-hours later by 0, 5, 16, or 32μg of DYD CA, followed one hour later by 2.4nmol of ^{90}Y-DOTA-Biotin. The greatest amount of radioactivity was present in the tumors of animals that received no CA (5.7±0.6%ID/g, Figure 3B). However, high levels of radioactivity were also observed in the blood (5.6±0.6%ID/g), lungs (2.9±0.1%ID/g), liver (1.3±0.1%ID/g), and kidneys (1.6±0.2%ID/g, unless DYD was administered (Figure 3B). All three doses of CA (5, 16, and 32μg) were highly effective in removing excess FP from the bloodstream (~98% clearance within 30 minutes) and in markedly diminishing the uptake of the ^{90}Y-radiolabeled construct in critical normal organs (Figure 3B), although the amount of radioactivity in tumor sites also dropped progressively with increasing amounts of CA. Hence, the lowest amount of CA (5μg) was selected as optimal for further experiments since it afforded the best compromise between effective clearance of bispecific Ab from the blood stream and normal organs, while retaining high levels of radioactivity in target tumor sites (Figure 3B).

Biodistributions of radioactivity with time

An experiment performed to evaluate the retention of radioactivity in tumor and normal organ sites as a function of time (Figure 4A) demonstrated selective targeting and retention of ^{90}Y in CD20-expressing tumor sites with high levels of radioactivity achieved within 4-hours of ^{90}Y-DOTA injection (13.8±1.4%ID/g), which persisted after 24-hours (10.4±1.5%ID/g), 48-hours (6.12±0.5%ID/g), and 120-hours (2.1±0.3%ID/g). Tumor-to-blood radioactivity ratios were 6:1 after 4-hours, 21:1 after 24-hours, 51:1 after 48-hours and 43:1 after 120-hours. Among normal organs, the lung retained the greatest amount of radioactivity (Figure 4A), presumably because of its high vascularity. Kidneys and liver retained much less radioactivity after 24-hours, (0.49±0.03%ID/g) and (0.53±0.05%ID/g) respectively, with tumor-to-organ ratios of 21:1 and 19:1, respectively. A non-binding CC49-Fc-C825 control FP showed no preferential retention in tumor sites, with a lower %ID/g in

tumor than in lungs at all time-points (Figure 4B). A comparative experiment was subsequently performed to assess the relative targeting of ^{90}Y-DOTA-biotin to tumor sites using bispecific 2H7-Fc-C825 PRIT compared to our previous "gold standard" PRIT approach using an anti-CD20-SA conjugate (1F5-SA). Virtually identical tumor targeting was observed with these two PRIT methods (8.4±.2%ID/g vs 8.2±1.0%ID/g, respectively after 24-hours; Figure 4C). However, the concentrations of ^{90}Y in the blood and normal organs were consistently higher with 1F-SA PRIT than with bispecific 2H7-Fc-C825 PRIT (e.g., for blood, 2.1±0.5%ID/g vs 0.6±0.1%; and for kidneys, 2.1±0.4%ID/g vs 0.6±0.1%, respectively). Consequently, tumor-to-organ ratios were considerably superior for bispecific PRIT compared to SA-biotin PRIT (e.g., tumor:blood, 14.8±3.5 vs. 4.4±1.6, p=0.0003; tumor:kidney, 15.3±2.6 vs. 4.2±1.1, p<0.0001, respectively). Very similar results were obtained in a separate experiment targeting the Granta xenografts (Figure 4D).

Dosimetry

Radiation absorbed doses to tumors, whole body, and 11 normal tissues were calculated for bispecific antibody PRIT using the methods described above (Table 1). The dosimetry method used accounted for organ self-dose absorbed fractions as well as beta-particle cross-organ dose contributions(34). The absorbed doses (cGy) per millicurie ^{90}Y administered, calculated from the ^{111}In tracer, showed tumor-to-normal organ ratios of 112:1 for the femur, 29:1 for the whole body, 25:1 for the kidneys, 21:1 for the blood, 6:1 for the liver, and 3:1 for the lung (Table 1).

Therapy Studies

Therapy studies were performed in athymic mice (n=10 mice per group) bearing subcutaneous Ramos or Granta-519^{luc} xenografts, using the optimal reagent concentrations and time-points for administration identified in the biodistribution studies. Four consecutive, concordant experiments demonstrated similar high levels of efficacy between bispecific antibody PRIT compared with SA-biotin PRIT when administered at equimolar doses (1.4nmol). In one representative experiment, escalating amounts of ^{90}Y-DOTA-biotin (14.8, 25.9, or 37MBq [400, 700, or 1000μCi]) were administered to mice bearing Ramos xenografts injected 24-hours earlier with 1.4nmol of 2H7-Fc-C825 bispecific Ab, 1F5-SA conjugate, or control reagents (CC49-Fc-C825 bispecific Ab or HB8181-SA conjugate). Dose-dependent inhibition of tumor growth (Figure 5A) and prolongation of mouse survival (Figure 5B) were dramatic with both CD20-pretargeted methods. All 30 mice in the three control groups and the 10 mice treated with 14.8MBq (400μCi) ^{90}Y-DOTA-biotin group died within 25 days, whereas 60–70% of mice treated with 25.9 MBq700 μCi) or 37MBq (1000μCi) of ^{90}Y-DOTA-biotin were cured, surviving tumor-free for the 150-day duration of the experiment (Figure 5A and 5B, p<0.0001, comparing any control or the 14.8MBq group to either the 25.9 or 37MBq group). The 1F5-SA conjugate possesses 4 binding sites for ^{90}Y-DOTA-biotin, whereas the 2H7-Fc-C825 bispecific Ab possess only 2 binding sites per molecule for ^{90}Y-DOTA-biotin. A subsequent experiment was therefore performed evaluating the potential benefit of administering twice the amount of 2H7-Fc-C825 Ab as 1F5-SA conjugate (2.8 vs 1.4nmol), followed by equivalent amounts of ^{90}Y-DOTA-biotin (37MBq [1000μCi], Figure 5C & 5D). In this experiment, 100% of animals treated with 2.8nmol of 2H7-Fc-C825 were cured compared with 50% of those with 1.4nmol of 1F5-SA

(Figure 5D, p=0.01), while treatment with 1.4nmol 2H7-Fc-C825 treatment was no better than with 1F5-SA (p=0.24). In this experiment, all 40 mice in 4 control groups died of progressive tumor growth before day 25 (Figure 5D).

Similarly encouraging efficacy of bispecific PRIT was demonstrated in an experiment in mice bearing Granta-519^{luc} xenografts where 90–100% of mice were cured with 25.9–37MBq (700–1000μCi) of ^{90}Y-DOTA-biotin (Figure 6A, 6B and 6C), sharply contrasting with the rapid tumor growth and death observed in all 20 mice in two control groups. (Figure 6A and 6B, p<0.0001).

Toxicity

PRIT was well tolerated at doses up to 37MBq (1000μCi) of ^{90}Y-DOTA-biotin, with negligible weight loss using either bispecific Ab or SA-biotin methods (Supplemental Figure S4). No significant evidence of renal or hepatic toxicity was observed by monitoring serial transaminase, alkaline phosphatase, blood urea nitrogen, or creatinine (not shown). Myelosuppression was minimal with bispecific Ab PRIT with very minor changes in the leukocyte, platelet, or red blood cell counts (Supplemental Figure S5). In contrast, SA-biotin PRIT produced more marked myleosuppression in three toxicity experiments. With SA-biotin PRIT, nadir WBC counts dropped to 10% of baseline, while with bispecific PRIT, the WBC dropped to 49% of baseline (p<0.0001). Hematocrits dropped to 52% of baseline with SA-biotin PRIT compared to 86% of baseline with bispecific PRIT (p<0.0001), and platelet counts dropped to 22% of baseline with SA-biotin PRIT compared to no decrement in platelets (100% of baseline) with bispecific PRIT (p<0.0001, Supplemental Figure S5).

DISCUSSION

Despite rapid advancements in the management of B cell malignancies using chemotherapeutic agents, monoclonal antibodies, RIT, and kinase inhibitors, approximately 25% of patients with NHL still succumb to the disease.(1) Anti-CD20 RIT is an underutilized modality that has a unique mechanism of action and the potential to eradicate disease in patients who are refractory to other forms of treatment when the therapeutic ratio is optimized. RIT with beta-particle emitting radioisotopes such as ^{90}Y kills tumor cells by inflicting multiple single strand (and to a lesser degree, double strand) DNA breaks. Multi-step PRIT is designed to overcome limitations associated with conventional directly radiolabeled antibody by facilitating dose escalation and enhancing efficacy. Many investigators have demonstrated the dramatic superiority of PRIT compared to conventional RIT in preclinical models(35–40). However, no comparative studies have been published rigorously comparing competing PRIT technologies to provide objective insight into the approach that should be preferentially translated into human clinical trials. This manuscript provides for the first time, to our knowledge, head-to-head comparisons of the two most widely used systems for pretargeting, namely SA-biotin and bispecific Ab PRIT. The SA-biotin approach has been widely tested and demonstrates striking efficacy, but has been criticized because SA is a highly immunogenic bacterial protein that may limit the ability to administer repeated cycles of therapy.(18, 41, 42) This potential limitation may be mitigated, however, in patients with hematologic malignancies, since their immunocompromised status

may render them incapable of responding to foreign immunogens. A second potential limitation of SA-biotin PRIT is the presence of endogenous biotin in the blood and tissues of patients, which theoretically could occupy SA binding sites, blocking binding of subsequently administered radio-biotin compounds. Several approaches have been proposed to circumvent the disadvantages of SA-biotin PRIT, including the genetic engineering of less immunogenic versions of SA(43, 44) and of mutant SA-molecules with a lower binding avidity for endogenous biotin, which nevertheless retain high avidity binding for synthetic, divalent radio-biotin ligands.(45–47) Despite these refinements to the SA-biotin PRIT approach, alternative methodologies are desirable. Bispecific Ab PRIT approaches appear particularly attractive, since they can easily be generated with non-immunogenic human or humanized antibodies and are not impacted by endogenous biotin.

In the studies described here, SA-biotin and bispecific approaches were both well tolerated, with minimal weight loss and no evidence of toxicity to normal organs in animals monitored for >150 days after ^{90}Y construct infusions up to 37MBq (1000μCi). Initial biodistribution experiments demonstrated tumor-to-kidney uptake ratios that were 5:1 24-hours after ^{90}Y-DOTA-biotin pretargeted by 1F5-SA (not shown). This finding was consistent with previous biodistribution experiments reported by our group demonstrating the kidney as the normal organ with the highest nonspecific radiation uptake after 1F5-SA-biotin PRIT (tumor-to-kidney ratios as low as 6:1 at 24-hours after the radiolabeled moiety was infused)(48). While no evidence of long term renal toxicity has been observed in SA-biotin PRIT therapy studies with infusions up to 44.4MBq (1200μCi)(49, 50), the kidney has represented the organ which would most likely define dose limiting toxicity in a SA-biotin PRIT clinical trial. In contrast, the biodistribution studies using 2H7-Fc-C825 PRIT described here demonstrate a tumor-to-kidney ratio of 21:1 after 24-hours (Figure 4A). This relative renal sparing may facilitate dose escalation in future clinical studies.

Myelosuppression was significantly more pronounced with SA-biotin PRIT (Supplemental Figure S5), presumably a consequence of the somewhat higher levels of blood radioactivity (Figure 4C and 4D) compared with that of bispecific PRIT. At day 14, the mice receiving 37MBq of ^{90}Y pretargeted by 2H7-Fc-C825 FP had WBC, HCT and platelet counts that were 49%, 100% and 86% of baseline respectively (Supplemental Figure S5) while those receiving the same amount of ^{90}Y using the SA-biotin approach had counts that were 10%, 22% and 52% of their baseline values ($p<0.0001$ for all comparisons to FP counts). In clinical settings, reduced myelosuppression may translate into lower rates of infection, fewer bleeding complications and improved outcomes. Moreover, while the incidence of secondary malignancies, including myelodysplastic syndrome, after conventional anti-CD20 RIT is not greater than that observed following other forms of chemotherapy(51) (3.5% following ^{131}I-tositumomab(51); 2.5% following ^{90}Y-ibritumomab tiuxetan(52)), the relative sparing of bone marrow from nonspecific radiation exposure after 2H7-Fc-C825 FP PRIT may reassure treating clinicians concerned about treatment associated myelotoxicity.

A potential limitation to PRIT treatment regimens is the inherent complexity that is unavoidable in a multi-step process. A potential advantage associated with bispecific PRIT is the relative simplicity of CA synthesis. Production of the DYD CA(28) involves straightforward chemistry that facilitates inexpensive large scale production. In contrast, the

SA-biotin system requires a synthetic N-acetyl-galactosamine CA consisting of a biotin joined through a modified aminocaproyl spacer to a core of a 4th generation dendrimeric backbone(53) and as consequence, production is more complex and costly.

Taken together, the results presented in this report confirm the highly specific targeting of radioactivity with both PRIT methods, although tumor-to-normal organ radioactivity ratios were superior with the bispecific approach. Therapeutic efficacy was similar with bispecific Ab and SA-biotin PRIT when the targeting first-step reagents were used at equimolar doses (1.4nmol), with 50–100% of animals cured with 37MBq (1000μCi) of ^{90}Y in four consecutive experiments using two different lymphoma xenograft models (e.g. Figure 5B). When the dose of 2H7-Fc-C825 was doubled to 2.8nmol to adjust for the difference in valency between the 1F5-SA conjugate (tetravalent binding to ^{90}Y-DOTA-biotin) and 2H7-Fc-C825 (bivalent binding to ^{90}Y-DOTA), the therapeutic efficacy was superior with the bispecific approach (Figure 5D).

In conclusion, both SA-biotin PRIT and bispecific Ab PRIT are safe and highly effective methods of curing mice bearing B cell lymphoma xenografts, but the bispecific Ab approach is preferred for future clinical trials because of a superior biodistribution profile, less myelosuppression, and improved efficacy when used at equivalent valency.

Supplementary Material

Refer to Web version on PubMed Central for supplementary material.

Acknowledgments

Financial Support: This work was supported by grants from the US National Institutes of Health NCI-K08CA151682 (DJG); NCI-R01CA076287 (O.W.P), NCI-R01CA136639 (OW.), NCI-R01CA154897 (OWP), NCI-K23CA154874 (BGT), K24CA184039 (AKG) and by the David and Patricia Giuliani Family Foundation.

References

1. Siegel RL, Miller KD, Jemal A. Cancer statistics, 2015. CA Cancer J Clin. 2015; 65:5–29. [PubMed: 25559415]
2. Advani RH, Buggy JJ, Sharman JP, Smith SM, Boyd TE, Grant B, et al. Bruton tyrosine kinase inhibitor ibrutinib (PCI-32765) has significant activity in patients with relapsed/refractory B-cell malignancies. Journal of clinical oncology : official journal of the American Society of Clinical Oncology. 2013; 31:88–94.
3. Gopal AK, Kahl BS, de Vos S, Wagner-Johnston ND, Schuster SJ, Jurczak WJ, et al. PI3Kdelta inhibition by idelalisib in patients with relapsed indolent lymphoma. The New England journal of medicine. 2014; 370:1008–18. [PubMed: 24450858]
4. Larson SM, Carrasquillo JA, Cheung NK, Press OW. Radioimmunotherapy of human tumours. Nature reviews Cancer. 2015; 15:347–60. [PubMed: 25998714]
5. Palanca-Wessels MC, Czuczman M, Salles G, Assouline S, Sehn LH, Flinn I, et al. Safety and activity of the anti-CD79B antibody-drug conjugate polatuzumab vedotin in relapsed or refractory B-cell non-Hodgkin lymphoma and chronic lymphocytic leukaemia: a phase 1 study. Lancet Oncol. 2015; 16:704–15. [PubMed: 25925619]
6. Witzig TE, White CA, Gordon LI, Murray JL, Wiseman GA, Emmanouilides C, et al. Final results of a randomized controlled study of the Zevalin radioimmunotherapy refimen versus a standard course of rituximab immunotherapy for B-cell NHL. Blood. 2000; 96:831a. (abstract 3591).

7. Kaminski MS, Tuck M, Estes J, Kolstad A, Ross CW, Zasadny K, et al. 131I-tositumomab therapy as initial treatment for follicular lymphoma. The New England journal of medicine. 2005; 352:441–9. [PubMed: 15689582]
8. Zinzani PL, Derenzini E, Pellegrini C, Rigacci L, Fabbri A, Gandolfi L, et al. Long-term efficacy and toxicity results of the FLUMIZ trial (fludarabine and mitoxantrone followed by yttrium-90 ibritumomab tiuxetan in untreated follicular lymphoma). Ann Oncol. 2012; 23:805–7. [PubMed: 22287683]
9. Press OW, Eary JF, Appelbaum FR, Martin PJ, Badger CC, Nelp WB, et al. Radiolabeled-antibody therapy of B-cell lymphoma with autologous bone marrow support. The New England journal of medicine. 1993; 329:1219–24. [PubMed: 7692295]
10. Fisher RI, Kaminski MS, Wahl RL, Knox SJ, Zelenetz AD, Vose JM, et al. Tositumomab and Iodine-131 Tositumomab Produces Durable Complete Remissions in a Subset of Heavily Pretreated Patients With Low-Grade and Transformed Non-Hodgkin's Lymphomas. Journal of clinical oncology : official journal of the American Society of Clinical Oncology. 2005; 23:7565–73. [PubMed: 16186600]
11. Press OW, Eary JF, Appelbaum FR, Martin PJ, Nelp WB, Glenn S, et al. Phase II trial of 131I-B1 (anti-CD20) antibody therapy with autologous stem cell transplantation for relapsed B cell lymphomas. Lancet. 1995; 346:336–40. [PubMed: 7623531]
12. Liu SY, Eary JF, Petersdorf SH, Martin PJ, Maloney DG, Appelbaum FR, et al. Follow-up of relapsed B-cell lymphoma patients treated with iodine-131-labeled anti-CD20 antibody and autologous stem-cell rescue. Journal of clinical oncology : official journal of the American Society of Clinical Oncology. 1998; 16:3270–8. [PubMed: 9779701]
13. Press OW, Eary JF, Gooley T, Gopal AK, Liu S, Rajendran JG, et al. A phase I/II trial of iodine-131-tositumomab (anti-CD20), etoposide, cyclophosphamide, and autologous stem cell transplantation for relapsed B-cell lymphomas. Blood. 2000; 96:2934–42. [PubMed: 11049969]
14. Nademanee A, Forman S, Molina A, Fung H, Smith D, Dagis A, et al. A phase 1/2 trial of high-dose yttrium-90-ibritumomab tiuxetan in combination with high-dose etoposide and cyclophosphamide followed by autologous stem cell transplantation in patients with poor-risk or relapsed non-Hodgkin lymphoma. Blood. 2005; 106:2896–902. [PubMed: 16002426]
15. Krishnan A, Nademanee A, Fung HC, Raubitschek AA, Molina A, Yamauchi D, et al. Phase II trial of a transplantation regimen of yttrium-90 ibritumomab tiuxetan and high-dose chemotherapy in patients with non-Hodgkin's lymphoma. Journal of clinical oncology : official journal of the American Society of Clinical Oncology. 2008; 26:90–5. [PubMed: 18025438]
16. Winter JN, Inwards DJ, Spies S, Wiseman G, Patton D, Erwin W, et al. Yttrium-90 ibritumomab tiuxetan doses calculated to deliver up to 15 Gy to critical organs may be safely combined with high-dose BEAM and autologous transplantation in relapsed or refractory B-cell non-Hodgkin's lymphoma. Journal of clinical oncology : official journal of the American Society of Clinical Oncology. 2009; 27:1653–9. [PubMed: 19255322]
17. Goodwin DA, Meares CF. Advances in pretargeting biotechnology. Biotechnol Adv. 2001; 19:435–50. [PubMed: 14538068]
18. Goldenberg DM, Sharkey RM, Paganelli G, Barbet J, Chatal JF. Antibody pretargeting advances cancer radioimmunodetection and radioimmunotherapy. Journal of clinical oncology : official journal of the American Society of Clinical Oncology. 2006; 24:823–34. [PubMed: 16380412]
19. Hnatowich DJ, Virzi F, Rusckowski M. Investigations of avidin and biotin for imaging applications. Journal of nuclear medicine : official publication, Society of Nuclear Medicine. 1987; 28:1294–302.
20. Axworthy DB, Fritzberg AR, Hylarides MD, Mallett RW, Theodore LJ, Gustavson LM, et al. Preclinical evaluation of an anti-tumor monoclonal antibody/streptavidin conjugate for pretargeted Y-90 radioimmunotherapy in a mouse xenograft model. Journal of immunotherapy. 1994:16.
21. Schultz J, Lin Y, Sanderson J, Zuo Y, Stone D, Mallett R, et al. A tetravalent single-chain antibody-streptavidin fusion protein for pretargeted lymphoma therapy. Cancer research. 2000; 60:6663–9. [PubMed: 11118050]
22. Zhang M, Yao Z, Garmestani K, Axworthy DB, Zhang Z, Mallett RW, et al. Pretargeting radioimmunotherapy of a murine model of adult T-cell leukemia with the alpha-emitting radionuclide, bismuth 213. Blood. 2002; 100:208–16. [PubMed: 12070029]

23. Chen X, Dou S, Liu G, Liu X, Wang Y, Chen L, et al. Synthesis and in vitro characterization of a dendrimer-MORF conjugate for amplification pretargeting. Bioconjug Chem. 2008; 19:1518–25. [PubMed: 18646837]
24. Liu G, Dou S, Yin D, Squires S, Liu X, Wang Y, et al. A novel pretargeting method for measuring antibody internalization in tumor cells. Cancer Biother Radiopharm. 2007; 22:33–9. [PubMed: 17461727]
25. Zeglis BM, Sevak KK, Reiner T, Mohindra P, Carlin SD, Zanzonico P, et al. A pretargeted PET imaging strategy based on bioorthogonal Diels-Alder click chemistry. J Nucl Med. 2013; 54:1389–96. [PubMed: 23708196]
26. Rossin R, Lappchen T, van den Bosch SM, Laforest R, Robillard MS. Diels-Alder Reaction for Tumor Pretargeting: In Vivo Chemistry Can Boost Tumor Radiation Dose Compared with Directly Labeled Antibody. J Nucl Med. 2013; 54:1989–95. [PubMed: 24092936]
27. Orcutt KD, Slusarczyk AL, Cieslewicz M, Ruiz-Yi B, Bhushan KR, Frangioni JV, et al. Engineering an antibody with picomolar affinity to DOTA chelates of multiple radionuclides for pretargeted radioimmunotherapy and imaging. Nuclear medicine and biology. 2011; 38:223–33. [PubMed: 21315278]
28. Orcutt KD, Rhoden JJ, Ruiz-Yi B, Frangioni JV, Wittrup KD. Effect of small-molecule-binding affinity on tumor uptake in vivo: a systematic study using a pretargeted bispecific antibody. Molecular cancer therapeutics. 2012; 11:1365–72. [PubMed: 22491799]
29. Press OW, Corcoran M, Subbiah K, Hamlin DK, Wilbur DS, Johnson T, et al. A Comparative Evaluation of Conventional and Pretargeted Radioimmunotherapy of CD20-expressing Lymphoma Xenografts. Blood. 2001; 98:2535–43. [PubMed: 11588052]
30. Pagel JM, Hedin N, Subbiah K, Meyer D, Mallet R, Axworthy D, et al. Comparison of anti-CD20 and anti-CD45 antibodies for conventional and pretargeted radioimmunotherapy of B-cell lymphomas. Blood. 2003; 101:2340–8. [PubMed: 12446461]
31. Green DJ, Orgun NN, Jones JC, Hylarides MD, Pagel JM, Hamlin DK, et al. A preclinical model of CD38-pretargeted radioimmunotherapy for plasma cell malignancies. Cancer research. 2014; 74:1179–89. [PubMed: 24371230]
32. Hui TE, Fisher DR, Kuhn JA, Williams LE, Nourigat C, Badger CC, et al. A mouse model for calculating cross-organ beta doses from yttrium-90-labeled immunoconjugates. Cancer. 1994; 73:951–7. [PubMed: 8306284]
33. Kaplan EL, Meier P. Nonparametric estimation from incomplete observations. J Am Stat Assoc. 1958; 53:457–81.
34. Hui TE, Fisher DR, Kuhn JA, Williams LE, Nourigat C, Badger CC, et al. A mouse model for calculating cross-organ beta doses from yttrium-90- labeled immunoconjugates. Cancer. 1994; 73:951–7. [PubMed: 8306284]
35. Frost SH, Back T, Chouin N, Hultborn R, Jacobsson L, Elgqvist J, et al. Comparison of 211At-PRIT and 211At-RIT of ovarian microtumors in a nude mouse model. Cancer biotherapy & radiopharmaceuticals. 2013; 28:108–14. [PubMed: 23230896]
36. Green DJ, Pagel JM, Nemecek ER, Lin Y, Kenoyer A, Pantelias A, et al. Pretargeting CD45 enhances the selective delivery of radiation to hematolymphoid tissues in nonhuman primates. Blood. 2009; 114:1226–35. [PubMed: 19515724]
37. Green DJ, Jones JC, Hylarides MD, Hamlin DK, Wilbur DS, Lin YK, et al. Anti-CD38 Pretargeted Radioimmunotherapy Eradicates Multiple Myeloma Xenografts In a Murine Model. Blood. 2013:122.
38. Pagel JM, Orgun N, Hamlin DK, Wilbur DS, Gooley TA, Gopal AK, et al. A comparative analysis of conventional and pretargeted radioimmunotherapy of B-cell lymphomas by targeting CD20, CD22, and HLA-DR singly and in combinations. Blood. 2009; 113:4903–13. [PubMed: 19124831]
39. Subbiah K, Hamlin DK, Pagel J, Wilbur DS, Meyer DL, Axworthy DB, et al. Comparative immunoscintigraphy, toxicity, and efficacy of conventional and pretargeted radioimmunotherapy in a CD20-expressing human lymphoma xenograft model. Journal of nuclear medicine : official publication, Society of Nuclear Medicine. 2003; 44:437–45.

40. Sharkey RM, Karacay H, Richel H, McBride WJ, Rossi EA, Chang K, et al. Optimizing bispecific antibody pretargeting for use in radioimmunotherapy. Clinical cancer research : an official journal of the American Association for Cancer Research. 2003; 9:3897S–913S. [PubMed: 14506188]
41. Paganelli G, Grana C, Chinol M, Cremonesi M, De Cicco C, De Braud F, et al. Antibody-guided three-step therapy for high grade glioma with yttrium- 90 biotin. European journal of nuclear medicine. 1999; 26:348–57. [PubMed: 10199940]
42. Goldenberg DM, Chang CH, Sharkey RM, Rossi EA, Karacay H, McBride W, et al. Radioimmunotherapy: is avidin-biotin pretargeting the preferred choice among pretargeting methods? European journal of nuclear medicine and molecular imaging. 2003; 30:777–80. [PubMed: 12574971]
43. Meyer DL, Schultz J, Lin Y, Henry A, Sanderson J, Jackson JM, et al. Reduced antibody response to streptavidin through site-directed mutagenesis. Protein science : a publication of the Protein Society. 2001; 10:491–503. [PubMed: 11344318]
44. Yumura K, Ui M, Doi H, Hamakubo T, Kodama T, Tsumoto K, et al. Mutations for decreasing the immunogenicity and maintaining the function of core streptavidin. Protein science : a publication of the Protein Society. 2013; 22:213–21. [PubMed: 23225702]
45. Park SI, Shenoi J, Frayo SM, Hamlin DK, Lin Y, Wilbur DS, et al. Pretargeted radioimmunotherapy using genetically engineered antibody-streptavidin fusion proteins for treatment of non-hodgkin lymphoma. Clin Cancer Res. 2011; 17:7373–82. [PubMed: 21976541]
46. Hamblett KJ, Kegley BB, Hamlin DK, Chyan MK, Hyre DE, Press OW, et al. A streptavidin-biotin binding system that minimizes blocking by endogenous biotin. Bioconjugate chemistry. 2002; 13:588–98. [PubMed: 12009950]
47. Hamblett KJ, Press OW, Meyer DL, Hamlin DK, Axworthy D, Wilbur DS, et al. Role of biotin-binding affinity in streptavidin-based pretargeted radioimmunotherapy of lymphoma. Bioconjugate chemistry. 2005; 16:131–8. [PubMed: 15656584]
48. Pantelias A, Pagel JM, Hedin N, Saganic L, Wilbur S, Hamlin DK, et al. Comparative biodistributions of pretargeted radioimmunoconjugates targeting CD20, CD22, and DR molecules on human B-cell lymphomas. Blood. 2007; 109:4980–7. [PubMed: 17303693]
49. Pagel JM, Matthews DC, Kenoyer A, Hamlin DK, Wilbur DS, Fisher DR, et al. Pretargeted radioimmunotherapy using anti-CD45 monoclonal antibodies to deliver radiation to murine hematolymphoid tissues and human myeloid leukemia. Cancer research. 2009; 69:185–92. [PubMed: 19118002]
50. Pagel JM, Lin Y, Hedin N, Pantelias A, Axworthy D, Stone D, et al. Comparison of a tetravalent single-chain antibody-streptavidin fusion protein and an antibody-streptavidin chemical conjugate for pretargeted anti-CD20 radioimmunotherapy of B-cell lymphomas. Blood. 2006; 108:328–36. [PubMed: 16556891]
51. Bennett JM, Kaminski MS, Leonard JP, Vose JM, Zelenetz AD, Knox SJ, et al. Assessment of treatment-related myelodysplastic syndromes and acute myeloid leukemia in patients with non-Hodgkin's lymphoma treated with Tositumomab and Iodine I 131 Tositumomab (BEXXAR(R)). Blood. 2005; 105:4576–82. [PubMed: 15731177]
52. Czuczman MS, Emmanouilides C, Darif M, Witzig TE, Gordon LI, Revell S, et al. Treatment-related myelodysplastic syndrome and acute myelogenous leukemia in patients treated with ibritumomab tiuxetan radioimmunotherapy. Journal of clinical oncology : official journal of the American Society of Clinical Oncology. 2007; 25:4285–92. [PubMed: 17709799]
53. Subbiah K, Hamlin DK, Pagel JM, Wilbur DS, Meyer DL, Axworthy DB, et al. Comparison of immunoscintigraphy, efficacy, and toxicity of conventional and pretargeted radioimmunotherapy in CD20-expressing human lymphoma xenografts. Journal of Nuclear Medicine. 2003; 44:437–45. [PubMed: 12621012]

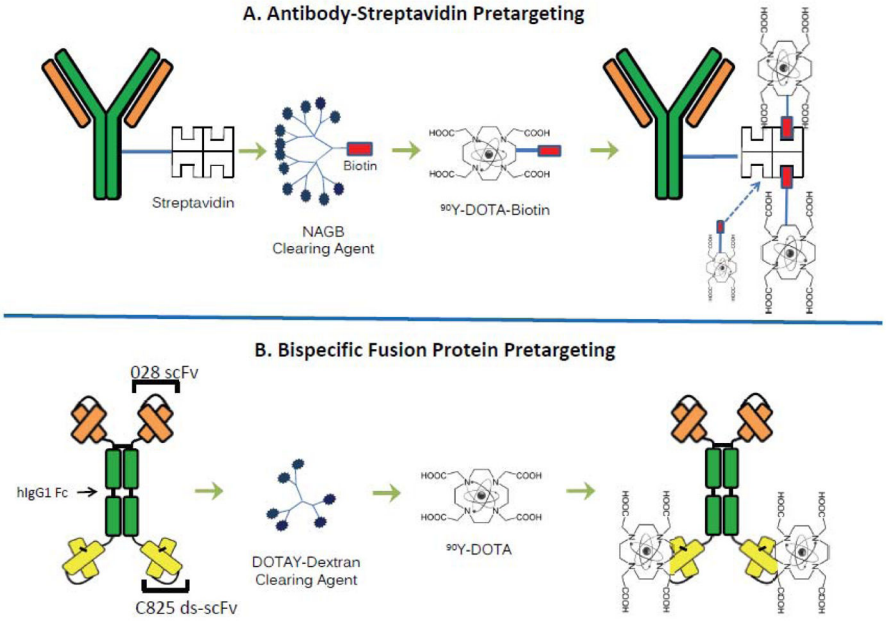

Figure 1.

Figure 1A,B. Schema comparing SA-biotin multistep pretargeted radioimmunotherapy (PRIT) (A) and 2H7-Fc-C825 bispecific FP PRIT (B). Infusion of the anti-CD20 construct is followed by injection of a synthetic CA (N-acetylgalactosamine or DOTAY-dextran) and then infusion of the radiolabeled small molecule.

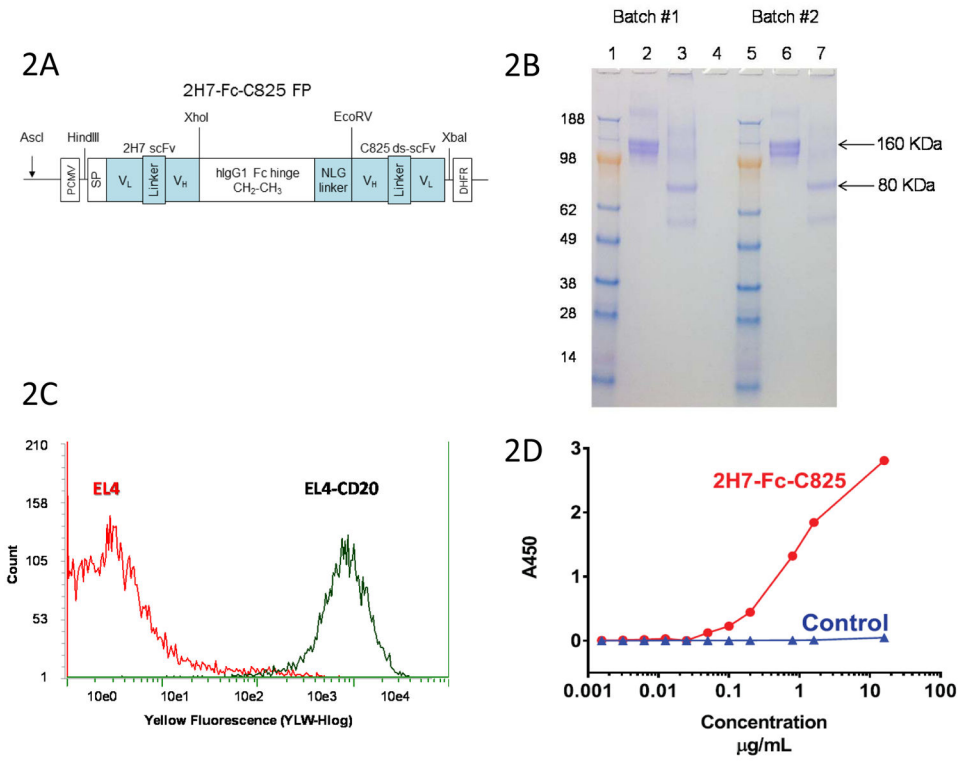

Figure 2.

Figure 2A. Schematic of the 2H7-Fc-C825 (anti-CD20 x anti-Y-DOTA) bispecific Fc fusion antibody gene. An anti-human CD20 2H7 scFv gene and an yttrium-DOTA capturing C825 disulfide-stabilized scFv (ds-scFv) gene were fused to the human IgG1 Fc fragment at the amino and carboxyl ends, respectively. An N-linked glycosylation containing linker (NLG) was incorporated between the Fc and C825 ds-scFv domains, as shown.

Figure 2B. SDS-PAGE analysis of the 2H7-Fc-C825 FP. Bispecific 2H7-Fc-C825 fusion polypeptides expressed in CHO-DG44 cells spontaneously formed dimers via the hinge regions. Two batches of 2H7-Fc-C825 FP (5µg) were analyzed by electrophoresis on a 4–20% MES SDS PAGE gel (Invitrogen). Lanes 1 and 5: Seeblue marker proteins; Lanes 2 and 6 show the non-reduced 2H7-Fc-C825 FP (samples boiled); Lanes 3 and 7 show the monomeric 2H7-Fc-C825 FP (samples boiled and reduced with 2-mercaptoethanol); Lane 4 is empty. The gel was stained with Coomassie blue.

Figure 2C. Flow Cytometric Analysis of Binding of Purified 2H7-Fc-C825 FP to cells transduced to express hCD20 (EL4-CD20, [black]) and to untransduced (control) EL4 cells (red). EL4 or EL4-CD20 cells ($0.5x10^6$ each) were incubated in 100µl of HBSS buffer containing 2% FBS and treated with 1.8µg of the 2H7-Fc-C825 FP for 30 min at 4°C. After washing, the cells were mixed with 2 µl of PE-anti-human Fc antibody in 40µl of HBSS-2% FBS buffer for 30 min at 4°C. After washing 3x,cells were re-suspended in 400µl of PBS buffer containing 1% of formaldehyde and analyzed on a Guava cytometer.

Figure 2D. Sandwich ELISA assay demonstrating concentration-dependent binding of the 2H7-Fc-C825 FP to microtiter wells coated with the Y-DOTA ligand. A 96-well plate was coated with 70µl of the BSA-Y-DOTA conjugate (1µg/ml in PBS) and then blocked with 200µl of 2% BSA in PBS buffer. After washing, the wells were treated with 100µl of fusion

proteins at a concentration of 16μg/ml followed by serial dilution as indicated. The plate was further treated with HRP-anti-human Fc antibody followed by TMB. A control FP shows no binding to Y-DOTA.

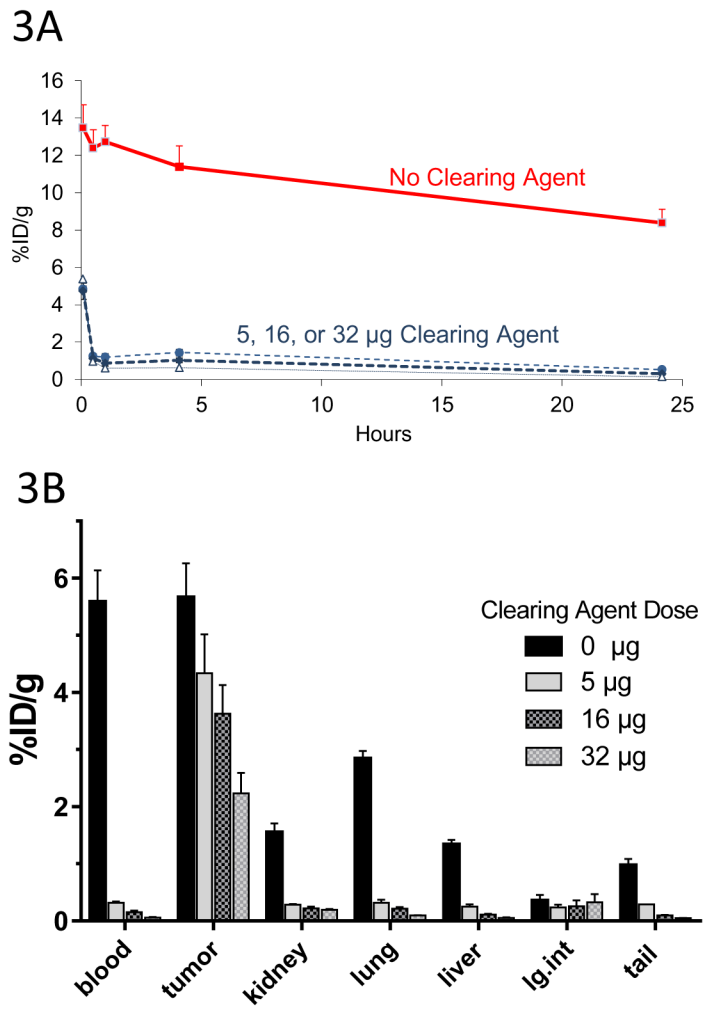

Figure 3. Optimization of DOTAY-Dextran CA Dose

Figure 3A. Blood clearance of circulating C825-Fc-2H7 FP by various doses of DOTAY-Dextran CA. Mice were injected with 1.4nmol of the 2H7-Fc-C825 fusion protein FP followed by 0, 5, 16 or 32µg of DOTAY-Dextran CA 23-hours later. One hour later, 2.4nmol of ^{90}Y-DOTA-Biotin was injected. Blood was collected after 0.08, 0.5, 1, 4, and 24-hours following injection of radioactivity. Results represent the calculated percentages of the injected dose per gram of tissue (%ID/g, ±SD; n=3) after corrections for decay and background subtraction (red square, diluent; filled circle, 5µg DYD; diamond, 16µg DYD; triangle, 32µg DYD).

Figure 3B. Biodistribution of ^{90}Y-DOTA-Biotin in organs of mice bearing subcutaneous Ramos xenografts following injection of various doses of DOTAY-Dextran CA. Mice were injected with 1.4nmol of 2H7-Fc-C825 followed by 0, 5, 16, or 32µg of DOTAY-Dextran CA 23-hours later. One hour after injection of DOTAY-Dextran, 2.4nmol of ^{90}Y-DOTA-Biotin was injected. Tissues were harvested 24-hours after the injection of radioactivity. Results represent the calculated mean percentages of the injected dose per gram of tissue (%ID/g, ±SEM; n=3) after corrections for decay and background.

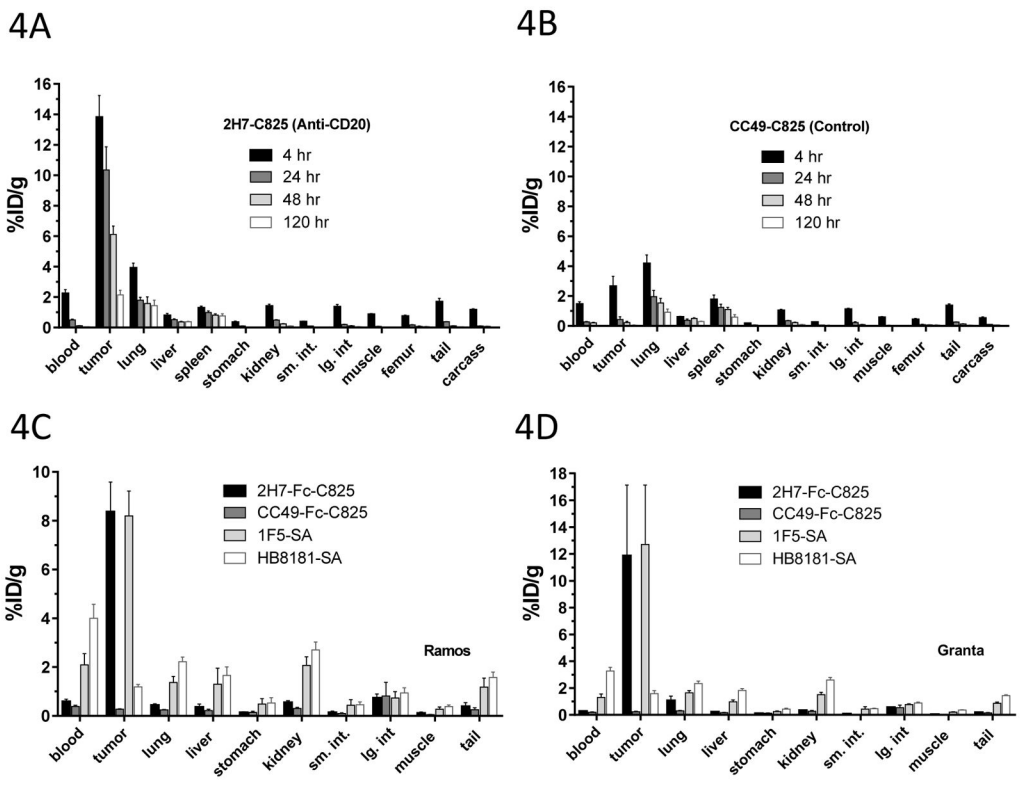

Figure 4.

Figure 4A,B. Biodistribution of ^{90}Y-DOTA-Biotin in mice bearing subcutaneous Ramos xenografts. Mice were injected with 1.4nmol of 2H7-Fc-C825 (A) or 1.4nmol of the control, non-binding CC49-Fc-C825 FP (B) followed by 5μg DOTAY-Dextran 23-hours later. One hour after the DOTAY-Dextran, 2.4nmol of ^{90}Y-DOTA-Biotin was injected. Tissues were harvested 4, 24, 48 and 120-hours after injection of radioactivity. Results represent the %ID/g (±SEM; n=5) after corrections for decay and background subtraction.

Figure 4C, D. Biodistribution of ^{90}Y-DOTA-Biotin in mice bearing subcutaneous Ramos xenografts (C) or Granta-519 xenografts. Mice were injected with 1.4nmol of 2H7-Fc-C825 (anti-CD20 bispecific), CC49-Fc-C825 (non-binding control bispecific antibody), 1F5-SA (anti-CD20-streptaviding conjugate) or HB8181-SA (non-binding control antibody-streptavidin conjugate), followed 23-hours later by either 5μg DOTAY-Dextran CA (for bispecific antibodies) or 5.8nmol NAGB CA (for antibody-streptavidin conjugates). One hour after injection of the CA, 2.4nmol of ^{90}Y-DOTA-Biotin was administered. Tissues were harvested 4, 24, 48 and 120-hours after injection of radioactivity. Results represent the calculated %ID/g(±SEM; n=5) after corrections for decay and background subtraction.

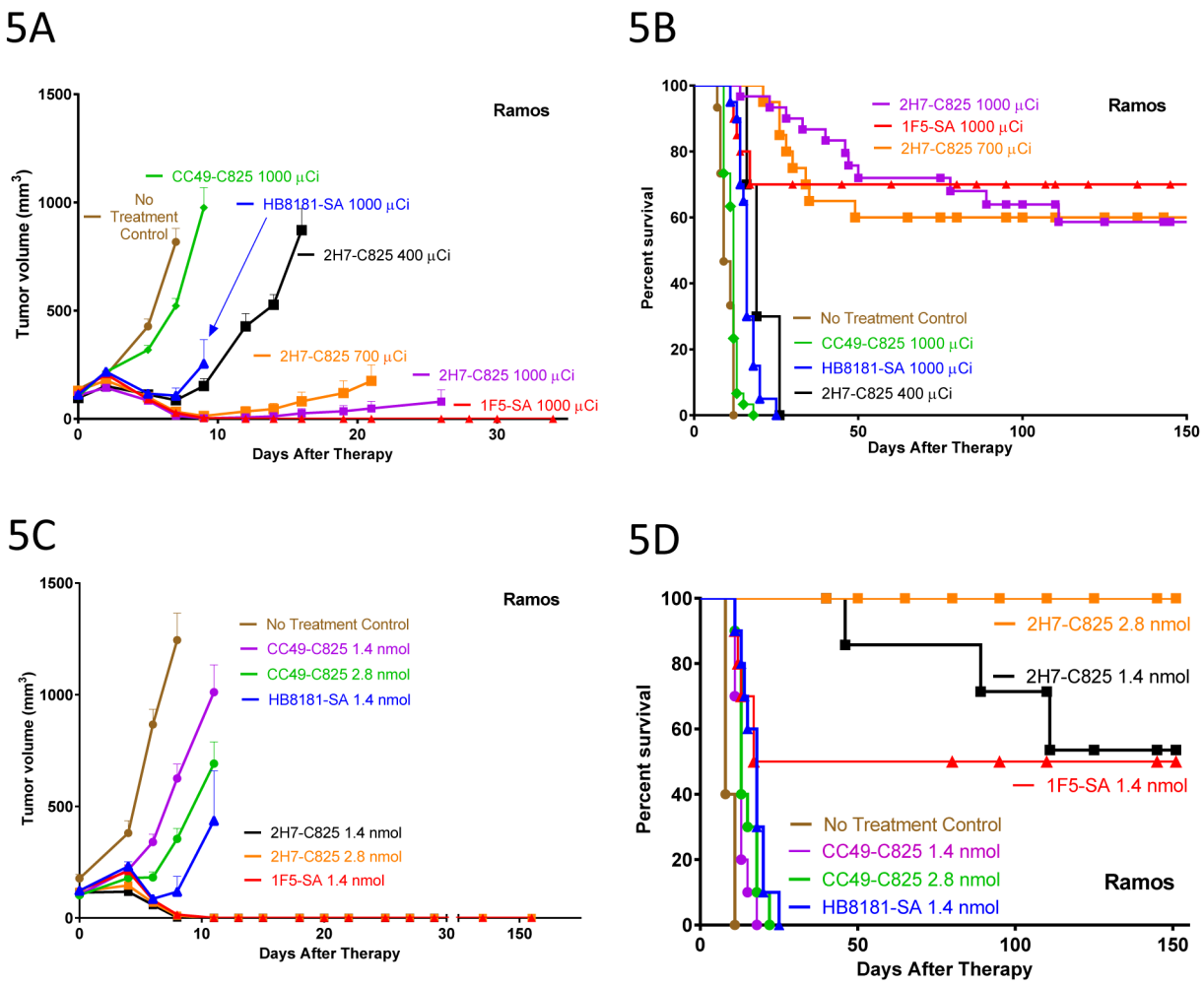

Figure 5.

Figure 5A, B. Comparison of tumor growth (A) and survival (B) in athymic mice bearing subcutaneous Ramos xenografts treated with either bispecific antibody PRIT or streptavidin-biotin PRIT. Mice were injected with 1.4nmol of 2H7-Fc-C825 (anti-CD20 bispecific), CC49-Fc-C825 (non-binding control bispecific antibody), 1F5-SA (anti-CD20-streptaviding conjugate) or HB8181-SA (non-binding control antibody-streptavidin conjugate), followed 23-hours later by either 5 µg DOTAY-Dextran CA (for bispecific antibodies) or 5.8 nmol NAGB CA (for antibody-streptavidin conjugates). One hour later, 2.4nmol DOTA-Biotin radiolabeled with various amounts of ^{90}Y was injected. Tumor growth results represent the mean tumor volume of Ramos xenografts (±SEM; brown, no treatment; green, 1000µCi ^{90}Y following 1.4 mol CC49-Fc-C825 ; blue, 1000µCi ^{90}Y following 1.4nmol HB8181-SA; red, 1000µCi ^{90}Y following 1.4nmol 1F5-SA; black, 400µCi ^{90}Y following 1.4nmol 2H7-Fc-C825 ; orange square, 700µCi ^{90}Y following 1.4nmol 2H7-Fc-C825 ; magenta, 1000µCi ^{90}Y following 1.4nmol 2H7-Fc-C825).

Figure 5C. Comparison of Tumor Growth of Ramos xenografts in Athymic mice injected with either 1.4 or 2.8nmol 2H7-Fc-C825 (anti-CD20 Bispecific Ab) or CC49-Fc-C825 (Control Bispecific Ab), 1.4nmol 1F5-SA (Anti-CD20-streptavidin conjugate), or 1.4nmol

HB8181-SA (control Ab-streptavidin conjugate), followed 23-hours later by either 5μg DOTAY-Dextran (for bispecific antibodies) or 5.8nmol NAGB (for Ab-streptavidin conjugates). One hour later 2.4nmol of ^{90}Y-DOTA-Biotin radiolabeled with 1000μCi was administered. Results represent the mean tumor volume of Ramos xenografts (±SEM; n=10; brown, no treatment; magenta, 1.4nmol CC49-Fc-C825 ; green, 2.8nmol CC49-FC-C825 ; black, 1.4nmol 2H7-Fc-C825 ; orange, 2.8nmol 2H7-Fc-C825 ; blue, 1.4nmol HB8181-SA; red, 1.4nmol 1F5-SA).

Figure 5D. Comparison of survival of athymic mice bearing subcutaneous Ramos xenografts treated with various doses of bispecific antibody PRIT or streptavidin-biotin followed by 1000μCi of ^{90}Y-DOTA-biotin. Mice were treated as described in the legend to figure 5A.

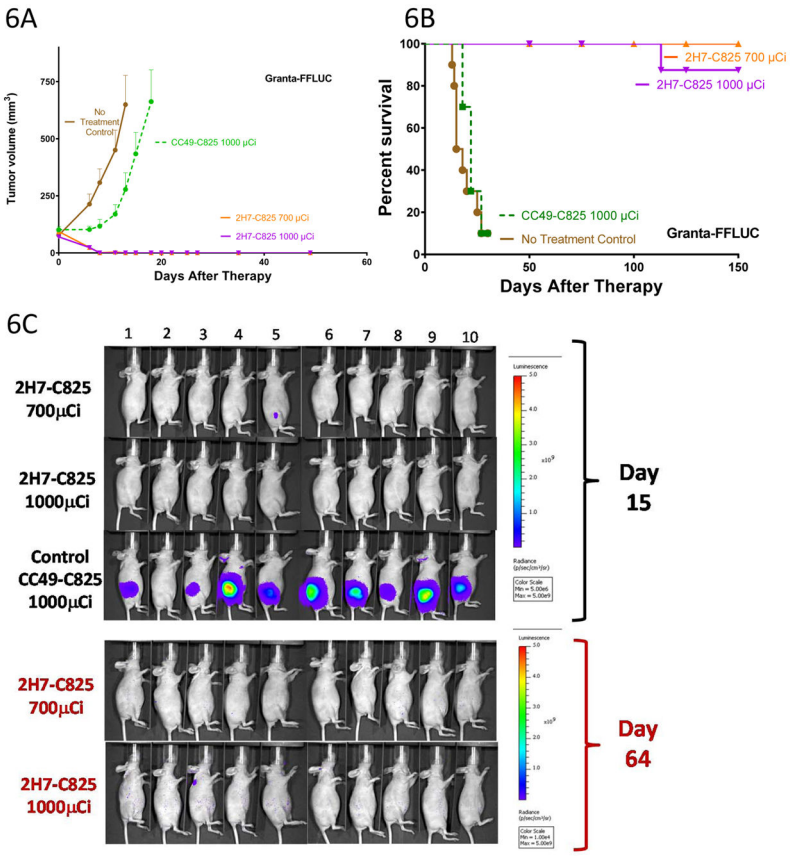

Figure 6.

Figure 6A, B. Tumor growth (A) and survival (B) n athymic mice bearing subcutaneous Granta-519^{luc} xenografts treated with bispecific Ab PRIT. Groups of 10 mice each were injected with 1.4nmol of either 2H7-Fc-C825 (Anti-CD20 bispecific) or CC49-Fc-C825 (control bispecific antibody) followed 23-hours later by 5µg of DOTAY-Dextran CA to remove excess circulating FP from the circulation. One hour later, 2.4nmol of ^{90}Y-DOTA-biotin radiolabeled with either 700 or 1000µCi of ^{90}Y was injected. Results represent the mean tumor volume of Granta-519^{luc} xenograft mice (±SEM; n=10; brown, no treatment control; green, 1000µCi ^{90}Y following 1.4nmol CC49-Fc-C825; orange, 700µCi ^{90}Y following 1.4nmol 2H7-Fc-C825 ; magenta, 1000µCi ^{90}Y following 1.4nmol 2H7-Fc-C825).

Figure 6C. Whole-body ventral BLI images (from mice treated as described in the legend to Figure 6A) obtained on day 15 (top) demonstrate signal corresponding with measurable disease in the left flank subcutaneous Granta-519^{luc} xenograft tumors of animals receiving nonbinding control FP (CC49-Fc-C825). At the same timepoint, no tumors were identified in mice pretargeted with 2H7-Fc-C825 followed by 1000µCi of ^{90}Y-DOTA-biotin, and one mouse in the treatment group receiving 700µCi of ^{90}Y-DOTA-biotin (animal #5) had measurable disease that was regressing. Day-64 imaging (bottom) of all surviving animals revealed no measurable disease. The imaging data were normalized to the same scale for each timepoint.

Table 1

Absorbed Radiation Doses

Tissue	2H7C825	CC49C825	T:N ratios for 2H7-C825	T:N ratios for CC49-C825
Blood	0.363	0.236	21.43	1.60
Lung	2.44	1.92	3.19	5.08
Liver	1.41	1.08	5.52	2.86
Spleen	1.51	1.1	5.15	2.91
Stomach	0.09	0.098	86.44	0.26
Kidneys	0.313	0.25	24.86	0.66
Small Intestine	0.101	0.122	77.03	0.32
Large Intestine	0.254	0.227	30.63	0.60
Muscle	0.205	0.125	37.95	0.33
Femur	0.069	0.112	112.75	0.30
Tail	0.121	0.094	64.30	0.25
Carcass	0.267	0.051	29.14	0.13
Tumor	7.78	0.378	1.00	1.00

Absorbed Dose/μCi

The methods are those described by Hui et al (Hui, TE, Fisher DR, Kuhn JA, Williams LE, Nourigat C, Badger CC, Beatty BG, Beatty JD. A Mouse Model for Calculating Cross-Organ Beta Doses from ^{90}Y-Labeled Immunoconjugates. Cancer 73(3Suppl):951–957, 1994). This method takes into account the beta particle absorbed fractions for small organs. The results are given as radiation absorbed dose (centigray) per unit administered activity (per microcurie).